Naval Research Laboratory
Washington, DC 20375-5320

NRL/MR/6410--01-8556

An Analysis of Lift-Off in Laminar Diffusion Flames

SALLY A. CHEATHAM
ELAINE S. ORAN

Laboratory for Computational Physics and Fluid Dynamics

June 11, 2001

REPORT DOCUMENTATION PAGE

Form Approved
OMB No. 0704-0188

1. AGENCY USE ONLY (*Leave Blank*)	2. REPORT DATE	3. REPORT TYPE AND DATES COVERED
	June 11, 2001	Interim

4. TITLE AND SUBTITLE

An Analysis of Lift-Off in Laminar Diffusion Flames

5. FUNDING NUMBERS

6. AUTHOR(S)

Sally A. Cheatham and Elaine S. Oran

7. PERFORMING ORGANIZATION NAME(S) AND ADDRESS(ES)

Naval Research Laboratory
Washington, DC 20375-5320

8. PERFORMING ORGANIZATION REPORT NUMBER

NRL/MR/6410--01-8556

9. SPONSORING/MONITORING AGENCY NAME(S) AND ADDRESS(ES)

Office of Naval Research
800 North Quincy Street
Arlington, VA 22217-5660

10. SPONSORING/MONITORING AGENCY REPORT NUMBER

11. SUPPLEMENTARY NOTES

12a. DISTRIBUTION/AVAILABILITY STATEMENT

Approved for public release; distribution is unlimited.

12b. DISTRIBUTION CODE

13. ABSTRACT (*Maximum 200 words*)

A jet diffusion flame attached to a burner rim may lift off and become stabilized further downstream when the jet velocity is sufficiently increased. In turbulent jet diffusion flames, such liftoff has been described alternately as the result of a stabilized premixed flame base, and as the result of extinguished diffusion flamelets at the flame base. Laminar flames exhibit liftoff behavior as well, and possess a relatively simpler flame structure which may be studied to provide insight into the basic mechanism responsible for flame lift. In the present study, an asymptotic solution and a numerical solution of a reduced set of equations are used to study the lifted structure of a laminar diffusion flame associated with a fuel jet. The numerical model solves a temperature equation with a finite chemical reaction rate. The asymptotic analysis is based on a flame-sheet model in the limit of large activation energy and large Damköhler number. While it is likely that premixing at the flame base affects the structure of a lifted flame, the current analysis suggests that local extinction of the flame at its base is a contributing mechanism to flame lift.

14. SUBJECT TERMS

Laminar diffusion flame
Flame extinction
Flame lift-off
Jet flame

15. NUMBER OF PAGES

27

16. PRICE CODE

17. SECURITY CLASSIFICATION OF REPORT	18. SECURITY CLASSIFICATION OF THIS PAGE	19. SECURITY CLASSIFICATION OF ABSTRACT	20. LIMITATION OF ABSTRACT
UNCLASSIFIED	UNCLASSIFIED	UNCLASSIFIED	UL

NSN 7540-01-280-5500

Standard Form 298 (Rev. 2-89)
Prescribed by ANSI Std 239-18
298-102

CONTENTS

AN ANALYSIS OF LIFT-OFF IN LAMINAR DIFFUSION FLAMES

INTRODUCTION

When the flow rate of a fuel jet is increased, a jet diffusion flame attached to a burner rim may lift off and become stabilized further downstream. Theories describing the stabilization of such lifted flames in turbulent flow regimes have postulated that the flame at its base is fully premixed and thus stabilized where the average axial velocity equals the mean burning velocity of the premixture [1], [2]. Other theories suggest that turbulent diffusion flames may be described as a collection of laminar flamelets, with liftoff occurring when a sufficient number of flamelets near the jet exit become extinguished due to excessive strain [3], [4]. An extensive review of such turbulent liftoff theories has been given by Pitts [5]. Laminar flames exhibit liftoff behavior as well, and have a relatively simpler flame structure which may be studied to provide insight into the basic mechanism responsible for flame lift. In the particular context of a fuel jet, lifted laminar flames have been observed both experimentally and numerically [6], [7]. Theoretical predictions of laminar flame liftoff heights have been obtained using cold jet theories in which the flame base is predicted to occur along stoichiometric contours where the flow velocity balances the velocity of a premixed flame base [8], [6], [9]. Wichman and Ramadan have used scaling arguments, and detailed comparisons to numerical solutions of the same equations, to elucidate liftoff trends [10]. Experimental and numerical studies which may be relevant to the flame structure at the base of a lifted flame include those of triple flames, often studied theoretically in the context of a stratified premixture [11], as well as those describing diffusion flame evolution in mixing layers [12] and phenomenological models of edge flames [13].

In the present study, the structure of a laminar diffusion flame associated with a fuel jet is analyzed to investigate flame lift. Here a Cartesian geometry is considered in which the two-dimensional planar fuel jet is surrounded by a coflow of oxidant of the same velocity. Two approaches are undertaken to describe such a flame. First, solutions are found by solving a reduced system numerically. Next, an asymptotic solution is constructed. The formulation of the asymptotic model is based on a flame sheet approximation, in a distinguished limit between large activation energy and large Damköhler number. Results of the two solution methods are compared and discussed. The effect of flow velocity as well as other parameters of the combustion field on the flame is investigated.

FORMULATION

The jet diffusion flame is modeled by a two-dimensional slot geometry, as shown in Figure 1. The half-width of the inner wall has been normalized to unity. In order to simulate an unconfined flame, the half width of the (normalized) outer boundary L is taken to be large so that the outer wall has a negligible effect on the combustion field. The chemical reaction is modeled as a global one-step reaction of the form

$$\nu_F F + \nu_X O \rightarrow P \tag{1}$$

where F, O and P represent the fuel, oxidant and product of the reaction, and ν_F, ν_X are the fuel and oxidant stoichiometric coefficients. An Arrhenius temperature dependence of the reaction has been assumed.

Manuscript approved April 30, 2001.

The resulting dimensionless, steady-state form of the governing equations reflecting conservation of energy and mass balance of the reactants is

$$m\frac{\partial T}{\partial x} - \frac{\partial^2 T}{\partial x^2} - \frac{\partial^2 T}{\partial y^2} = D\rho^2 Y_F Y_O e^{-\theta/T} \tag{2}$$

$$m\frac{\partial Y_F}{\partial x} - \frac{\partial^2 Y_F}{\partial x^2} - \frac{\partial^2 Y_F}{\partial y^2} = -D\rho^2 Y_O Y_F e^{-\theta/T} \tag{3}$$

$$m\frac{\partial Y_O}{\partial x} - \frac{\partial^2 Y_O}{\partial x^2} - \frac{\partial^2 Y_O}{\partial y^2} = -D\rho^2 Y_O Y_F e^{-\theta/T} \tag{4}$$

Here it has been assumed that the velocity profile is one-dimensional,

$$\mathbf{v} = (u, 0, 0) \tag{5}$$

so that, from the continuity equation, the mass flux $m = \rho u$=constant. The momentum equation is thus decoupled from the system and can be solved a posteriori to determine the small deviation from the constant, time-independent ambient pressure. The equation of state is given by $\rho T = 1$.

In the above equations, lengths have been made dimensionless by the half width of the fuel slot a, and velocity by the diffusional velocity $u_D = \lambda/\rho_c c_p a$. Here c_p is an averaged constant specific heat of the mixture, and λ is the thermal conductivity. A reference value $\rho_c = p_c \bar{W}/R_0 T_c$ is used to make the density dimensionless, where p_c is the ambient pressure, $\bar{W}$ is an averaged molecular weight of the mixture, and R_0 is the gas constant. The temperature T has been scaled by $T_c = (Q/c_p)(Y_{FJ}/\nu_F W_F)$, the fuel mass fraction by its initial value at the slot exit Y_{FJ}, and the oxidant mass fraction has been scaled by $Y_{FJ}(\nu_X W_X/\nu_F W_F)$. Here Q is the heat release, and W_F and W_X are the fuel and oxidant molecular weights, respectively. Unity Lewis numbers have been assumed, so that $\lambda/\rho c_p D_F = \lambda/\rho c_p D_X = 1$ where D_F and D_X are fuel and oxidant mass diffusivities. Then the Damköhler number $D = \nu_X Y_{FJ} B \rho_c a/W_F u_D$, where B is a pre-exponential factor of the reaction, and the scaled activation energy $\theta = E/R_0 T_c$.

The configuration is symmetric with respect to y, so that it suffices to solve the system on the half-space $0 \le y \le L$. Boundary conditions reflecting symmetry at $y = 0$ and no-flux conditions at $y = L$ are

$$\frac{\partial T}{\partial y} = \frac{\partial Y_F}{\partial y} = \frac{\partial Y_O}{\partial y} = 0. \tag{6}$$

At $x = 0$, boundary conditions are

$$mY_O - \frac{\partial Y_O}{\partial x} = 0, \quad mT - \frac{\partial T}{\partial x} = mT_J, \quad mY_F - \frac{\partial Y_F}{\partial x} = m \quad \text{for } 0 < y \le 1 \tag{7}$$

$$mY_O - \frac{\partial Y_O}{\partial x} = mX_{O0}, \quad mT - \frac{\partial T}{\partial x} = mT_{O0}, \quad mY_F - \frac{\partial Y_F}{\partial x} = 0 \quad \text{for } 1 < y \le L, \tag{8}$$

where T_J and T_{O0} are the (dimensionless) temperatures of the fuel and oxidant at their sources, respectively. The dimensionless oxidant source mass fraction is X_{O0} and the scaled fuel source mass fraction is unity. Boundedness of solutions is required as $x \to \infty$.

Before proceeding to finding solutions of the above equations, we note the existence of coupling functions which satisfy a reaction-free form of the governing equations. In particular,

$$\mathbf{L}(T + Y_F) = \mathbf{L}(T + Y_O) = \mathbf{L}(Y_F - Y_O) = 0 \tag{9}$$

where

$$\mathbf{L} \equiv m\frac{\partial}{\partial x} - \frac{\partial^2}{\partial x^2} - \frac{\partial^2}{\partial y^2}. \tag{10}$$

Applying the boundary conditions of Eqs. 6-8 one thus finds solutions

$$T + Y_F = \frac{1 + T_J + T_{O0}(L-1)}{L} + [1 + T_J - T_{O0}]S(x,y) \tag{11}$$

$$T + Y_O = \frac{T_J + (T_{O0} + X_{O0})(L-1)}{L} + [T_J - T_{O0} - X_{O0}]S(x,y) \tag{12}$$

$$Y_F - Y_O = \frac{1 + X_{O0}(1-L)}{L} + [1 + X_{O0}]S(x,y) \tag{13}$$

where

$$S(x,y) = \sum_{n=1}^{\infty} \frac{4m}{n\pi(m + \sqrt{m^2 + 4(n\pi/L)^2})} \sin\left(\frac{n\pi}{L}\right) \cos\left(\frac{n\pi y}{L}\right) \exp\left(\frac{m - \sqrt{m^2 + 4(n\pi/L)^2}}{2} x\right);$$

in calculating $S(x,y)$, we truncate the infinite series to a finite series over N modes. The above solutions will prove useful in simplifying the analysis which follows.

NUMERICAL FORMULATION

To begin to explore laminar flame lift, we numerically solve a time-dependent form of the system Eqs. 2-8 and march to a steady state. The coupling functions Eqs. 11-12 may be used to express Y_F and Y_O in terms of T, so that solving the system requires only the solution of the temperature equation

$$\rho \frac{\partial T}{\partial t} + m \frac{\partial T}{\partial x} - \frac{\partial^2 T}{\partial x^2} - \frac{\partial^2 T}{\partial y^2} = D\rho^2 Y_F Y_O e^{-\theta/T}, \tag{14}$$

subject to the boundary condition at $x = 0$

$$\text{for } 0 \le y \le 1, \quad mT - \frac{\partial T}{\partial x} = mT_J; \quad \text{for } 1 \le y \le L, \quad mT - \frac{\partial T}{\partial x} = mT_{O0} \tag{15}$$

and the condition at $x = x_{max}$,

$$\frac{\partial T}{\partial x} = 0. \tag{16}$$

At $y = 0$ and $y = L$,

$$\frac{\partial T}{\partial y} = 0. \tag{17}$$

Equation 14 is solved using a flux-corrected transport method. The liftoff height is calculated numerically as the $x-$location where the temperature at some y first reaches a threshold temperature T_{liftoff} defined as

$$T_{\text{liftoff}} = T_{\text{amb}} + \frac{T_f - T_{\text{amb}}}{2}. \tag{18}$$

Here the ambient temperature T_{amb} is defined as the maximum of the fuel and oxidant source temperatures, $T_{\text{amb}} = \max(T_J, T_{O0})$; T_f is the flame temperature corresponding to complete combustion. The flame height in the numerical calculations is defined to be the x-location where the temperature reaches a maximum value at the centerline $y = 0$. Convergence to a steady state was determined primarily from the convergence of the flame liftoff height. Convergence tests were also performed with respect to grid discretization and timestep size.

Numerical Solutions

Typical profiles resulting from the solution of Eqs. 14-17 are shown in Figure 2. Here $T_J = T_{O0} = 0.1$, $X_{O0} = 1.0$, $D = 4 \times 10^7$, and $\theta = 5.0$. The liftoff height in Figure 2 is calculated to be $x_{\ell h} = 2.85$, and the flame height is $x_{fh} = 9.93$.

In Figure 3, liftoff heights versus flow rate m are shown for several values of the Damköhler number D. Here $T_J = T_{O0} = 0.1$, $X_{O0} = 1.0$, and $\theta = 5.0$. In this figure, the liftoff height exhibits a threshold phenomenon with respect to the flow rate parameter m. The flame appears to remain attached until a sufficiently large value of m is reached; as m is increased beyond this value the liftoff height increases at a faster-than-linear rate. Calculated flame heights are also shown in Figure 3, and increase linearly with flow rate m.

In Figure 4, liftoff heights are shown for several values of m as a function of the Damköhler number. Here, as in Figure 3, $T_J = T_{O0} = 0.1$, $X_{O0} = 1.0$, and $\theta = 5.0$. Figure 4 again indicates the trend that as the Damköhler number decreases, liftoff heights increase for a fixed value of m. Furthermore, at a given value of D, liftoff heights are higher for larger values of m.

In Figure 5, temperature profiles are shown for three values of the flow rate m. Here $T_J = T_{O0} = 0.1$, $X_{O0} = 1.0$, $D = 4\times10^7$, $\theta = 5.0$. In Figure 6, corresponding maps of the reaction rate $\rho^2 D Y_F Y_O e^{-\theta/T}$ are shown. As m is increased, the flame evolves from a Burke-Schumann type attached flame, to a lifted flame with triple flame structures at its base, to a higher, lifted, curved horizontal flame front.

ASYMPTOTIC ANALYSIS

While the numerical results show us that even a simple model of a jet diffusion flame shows flame lift, our numerical results do not show *how* flames are stabilized. In trying to understand this, we first briefly analyze our results in terms of the simplest premixed stabilization theory, which suggests that a flame is stabilized where the cold flow velocity equals a premixed burning velocity. Chung and Lee [20], for example, consider similarly simplified governing equations but for an axisymmetric jet geometry without a coflow. They obtain liftoff heights by determining where the cold flow velocity contour representing an appropriate premixed burning velocity intersects the stoichiometric concentration contour. We may attempt to apply this methodology to the present problem in order to determine liftoff heights. Since we have assumed a one-dimensional velocity field, the cold flow velocity in our model is constant everywhere in the flow field. Then the fully premixed stabilization theory suggests that we should find a stabilized flame for only a single jet velocity (the appropriate premixed burning velocity), with the liftoff height for this velocity being indeterminate since the cold flow velocity is the same everywhere in the flow field. Contrary to this, however, we find stabilized lifted flames for a continuum of jet velocities with an apparently unique lift off height for each jet velocity. This suggests that the mechanism is more complicated. In an attempt to gain further insight into the stabilization mechanism, we therefore turn to theory.

Specifically, we return to Eqs. 2-4, 6-8 and seek an asymptotic solution in a distinguished limit of large activation energy θ and large Damköhler number D. Variables are expanded as

$$T \sim T_0 + \epsilon T_1 + \cdots \tag{19}$$

$$Y_F \sim Y_{F0} + \epsilon Y_{F1} + \cdots \tag{20}$$

$$Y_O \sim Y_{O0} + \epsilon Y_{O1} + \cdots \tag{21}$$

where $\epsilon = T_f^2/\theta$ is an inverse activation energy parameter, with T_f the flame temperature. Solutions corresponding to a near extinction regime in which fuel and oxidant are nearly completely consumed at the flame will be sought. In such a limit chemical reaction is confined to a thin zone, to be

determined from the analysis. This "surface" of chemical reaction will be denoted by $F(x,y)=0$. To leading order, we assume that the flame separates a region of no oxidant ($F>0$) from a region where there is no fuel ($F<0$). The nonlinear chemical reaction terms in Eqs. 2-4 will thus be replaced by conditions at the flame front determined by an appropriate analysis of the reaction zone structure.

The governing equations to be solved at each order are then

$$m\frac{\partial T}{\partial x}-\frac{\partial^2 T}{\partial x^2}-\frac{\partial^2 T}{\partial y^2}=0 \tag{22}$$

$$m\frac{\partial Y_F}{\partial x}-\frac{\partial^2 Y_F}{\partial x^2}-\frac{\partial^2 Y_F}{\partial y^2}=0 \tag{23}$$

$$m\frac{\partial Y_O}{\partial x}-\frac{\partial^2 Y_O}{\partial x^2}-\frac{\partial^2 Y_O}{\partial y^2}=0 \tag{24}$$

which, again, are to be solved separately for $F>0$ and $F<0$, subject to the boundary conditions Eqs. 6-8, and conditions at the flame front

$$Y_{F0}=0 \text{ for } F<0,\ \ Y_{O0}=0 \text{ for } F>0. \tag{25}$$

$$[T_0]=[Y_{F0}]=[Y_{O0}]=0 \tag{26}$$

$$\left[\frac{\partial T_0}{\partial n}\right]=-\left[\frac{\partial Y_{F0}}{\partial n}\right]=-\left[\frac{\partial Y_{O0}}{\partial n}\right] \tag{27}$$

$$[T_1] = -[Y_{F1}]=-[Y_{O1}] \tag{28}$$

$$\left[\frac{\partial T_1}{\partial n}+\frac{\partial Y_{F1}}{\partial n}\right] = 0, \quad \left[\frac{\partial T_1}{\partial n}+\frac{\partial Y_{O1}}{\partial n}\right]=0 \tag{29}$$

$$Y_{F1}|_{F=0^+}=S_F \qquad Y_{O1}|_{F=0^-}=S_X. \tag{30}$$

Here jump conditions were obtained by integrating across the reaction zone [24]; brackets indicate the jump in the enclosed quantity from $F=0^-$ to $F=0^+$, where the normal derivative and unit normal vector are given by

$$\frac{\partial}{\partial n}=\mathbf{n}\cdot\nabla \qquad \text{and} \qquad \mathbf{n}=\frac{\nabla F}{|\nabla F|}. \tag{31}$$

In Eq. 30, S_F and S_X quantify the small amount of fuel and oxidant that leak through the flame as a result of departure from complete combustion at $\mathcal{O}(\epsilon)$. These quantities are determined from solutions of the flame front inner structure equation, to be discussed below. The above conditions are sufficient to determine T, Y_F, Y_O to $\mathcal{O}(\epsilon)$, as well as the flame position $F(x,y)=0$.

In general the above system is a free boundary problem which must be solved numerically. However, the existence of the coupling functions Eqs. 11-13 allows analytical solutions to be written for the leading order system. Regardless of the magnitude of the chemical reaction, if at the flame sheet fuel and oxidant to leading order are completely consumed, the flame must be located where $Y_F=Y_O\sim 0$. Then from Eq. 13, the flame position is given by

$$F(x,y)\equiv\frac{1+X_{O0}(1-L)}{L}+(1+X_{O0})S(x,y)=0 \tag{32}$$

Resulting flame shapes for a similar flow configuration have been discussed previously in [14]. The determination of the flame sheet now allows T_0, Y_{F0}, Y_{O0} to be calculated everywhere in the

combustion field from the coupling relations Eqs. 11-13, by substituting in the expansions Eqs. 19-21 and setting $Y_{F0} = 0$ in $F < 0$ and $Y_{O0} = 0$ in $F > 0$ appropriately. The adiabatic flame temperature may also be calculated from Eq. 11 or 12,

$$T_f = \frac{T_{O0} + X_{O0}(1 + T_J)}{1 + X_{O0}}. \tag{33}$$

Thus by exploiting the use of coupling functions and assuming near complete combustion at the flame, leading order solutions can be determined without recourse to a fully numerical solution of the free boundary problem. Leading order conditions at the flame and the flame boundary itself are also now known and can be summarized as

$$\text{at } F = 0^- \text{ and } F = 0^+, \;\; T_0 = T_f, \;\; Y_{F0} = 0, \;\; Y_{O0} = 0 \tag{34}$$

where $F(x, y)$ and T_f are given by Eqs. 32 and 33.

Proceeding to $\mathcal{O}(\epsilon)$, corrections to the leading order solution are sought in which departure from complete combustion is possible. Introducing the expansions Eqs.19-21 into the coupling function relations Eqs.11-13 gives

$$T_1 + Y_{F1} = 0, \;\; T_1 + Y_{O1} = 0, \;\; Y_{F1} - Y_{O1} = 0 \tag{35}$$

so that jump conditions (28) are satisfied automatically, and

$$\text{at } F = 0^- \;, \;\; -T_1 = Y_{F1} = Y_{O1} = S_F \tag{36}$$

$$\text{at } F = 0^+ \;, \;\; -T_1 = Y_{F1} = Y_{O1} = S_X. \tag{37}$$

Analysis of the reaction zone structure will provide S_F and S_X, the fuel and oxidant leakage through the flame. More significantly in the present context, such an analysis will provide important information regarding flame extinction.

Flame Front Inner Structure

To examine the reaction zone of the flame, coordinates are stretched at $F = 0$ and inner expansions are introduced of the form

$$T \sim T_f + \epsilon\tau_1 + \cdots \tag{38}$$

$$Y_F \sim \epsilon y_f + \cdots \tag{39}$$

$$Y_O \sim \epsilon y_o + \cdots \tag{40}$$

Substituting these expansions into the governing equations and performing an appropriate coordinate transformation, one finds that the equation for the temperature perturbation can be written in a form first given by Liñan [15] as

$$\frac{\partial^2 \phi}{\partial \zeta^2} = (\phi^2 - \zeta^2) \exp[-\delta_0^{-1/3}(\phi + \gamma\zeta)] \tag{41}$$

where ζ is a stretched coordinate normal to the flame surface. Boundary conditions are

$$\text{as } \zeta \to -\infty \quad \frac{\partial \phi}{\partial \zeta} = -1, \qquad \text{as } \zeta \to \infty \quad \frac{\partial \phi}{\partial \zeta} = 1. \tag{42}$$

The conditions at the flame front Eq. 30 then follow from the matching relations

$$S_X = \delta^{-1/3} \lim_{\zeta \to -\infty} (\phi + \zeta) \qquad S_F = \delta^{-1/3} \lim_{\zeta \to +\infty} (\phi - \zeta). \tag{43}$$

The reactant leakage at the flame sheet thus depends on two parameters, γ and δ, which follow from the coordinate transformation and are given by

$$\gamma = \frac{\left.\frac{\partial T_0}{\partial n}\right|_{n=0+} + \left.\frac{\partial T_0}{\partial n}\right|_{n=0-}}{\left.\frac{\partial T_0}{\partial n}\right|_{n=0-} - \left.\frac{\partial T_0^+}{\partial n}\right|_{n=0+}} \tag{44}$$

$$\delta = \frac{4D\epsilon^3 e^{-\theta/T_f}}{T_f^2 \left[\frac{\partial T_0}{\partial n}\right]^2}. \tag{45}$$

The parameter γ is a ratio of the excess heat transported to one side of the flame to the total heat generated at the flame. The limit of nearly complete combustion considered here implies that $-1 \leq \gamma \leq 1$. When $|\gamma| > 1$ there is a heat flux from the ambient to the flame, and, correspondingly, $\mathcal{O}(1)$ rather than $\mathcal{O}(\epsilon)$ leakage of fuel or oxidant occurs through the reaction zone; such a limit will not be discussed in this work. For the particular configuration considered here, we find

$$\gamma = \frac{2(T_J - T_{O0}) + (1 - X_{O0})}{(1 + X_{O0})}. \tag{46}$$

The parameter δ appearing in Eq. 41 is a reduced Damköhler number, and thus a measure of the completeness of the reaction. The limit $\delta \to \infty$ corresponds to the Burke-Schumann limit ($D \to \infty$) of complete combustion, in which $S_F = S_X = 0$. Numerical solution of Eqs. 41-42 indicates that, for moderate values of δ, the system Eqs. 41-42 has two physically relevant solutions; two different quantities of the reactant leakage are possible. However, as δ is decreased further, there exists a critical value δ_c, below which no solutions to Eqs. 41-42 exist. This value of δ_c depends solely on γ. Liñán [15] provides an approximation for δ_c based on numerical computations as

$$\delta_c = \exp(1.0)[(1 - |\gamma|) - (1 - |\gamma|)^2 + 0.26(1 - |\gamma|)^3 + 0.055(1 - |\gamma|)^4] \tag{47}$$

This implies that portions of the flame sheet where $\delta < \delta_c$, or

$$\left[\frac{\partial T_0}{\partial n}\right]^2 > \frac{4\epsilon^3 D e^{-\theta/T_f}}{T_f^2 \delta_c} \tag{48}$$

are extinguished.

From the leading order solutions derived from Eqs.11-13, the jump of the normal derivative of the temperature across the reaction zone is given by

$$\left[\frac{\partial T_0}{\partial n}\right]^2 = (1 + X_{O0})^2 \left(\left(\frac{\partial S}{\partial x}\right)^2 + \left(\frac{\partial S}{\partial y}\right)^2 \right)\Bigg|_{F=0}. \tag{49}$$

Parenthetically, we note that this quantity is essentially the scalar dissipation rate found when a mixture fraction formulation is used for the analysis. Evaluating this quantity we find that δ varies continuously along the flame sheet, attaining its minimum value at the flame base. Therefore, for

moderate values of $\Lambda = 4\epsilon^3 De^{-\theta/T_f}/T_f^2$, extinction of the flame near the flame base occurs below $x = x_c$ where $\delta(x_c) = \delta_c$.

When a portion of the flame sheet is thus extinguished, modification of the leading order solution is required. No longer are there two distinct regions of the flow field; in some regions fuel and oxidant coexist even at leading order. Nonetheless, chemical reaction in these regions will be negligible if the temperature is sufficiently low. To modify the preceding formulation to account for such a region, the condition Eq. 25 may be relaxed to

$$\text{at } F = 0^-, \ Y_{F0} = 0, \quad \text{at } F = 0^+, \ Y_{O0} = 0. \tag{50}$$

where the flame sheet location $F(x, y) = 0$ is now implied to exist only where $\delta \geq \delta_c$. This relaxation of the constraint Eq. 25 does not affect the validity of the preceding formulation if

$$\text{at } F = 0^-, \ \frac{\partial Y_F}{\partial n} = \mathcal{O}(\epsilon), \quad \text{and at } F = 0^+, \ \frac{\partial Y_O}{\partial n} = \mathcal{O}(\epsilon). \tag{51}$$

For D sufficiently large such that no portion of the flame sheet is extinguished, applying the constraint Eq. 50 results in the solution obtained by applying Eq. 25, with Eq. 51 being trivially satisfied. If the constraint 51 is not met, the formulation must be adjusted and one expects a modification of the extinction criteria Eq. 48.

When solving the asymptotic system under the assumption 51, for moderate values of D one must in general still resort to a fully numerical solution of the problem. In this case the region of pure mixing at the base of the flame will likely modify the temperature gradients at the edge of the flame, and thus the reduced Damköhler number δ, and flame position, now defined as where $Y_{F0} = Y_{O0} = 0$ *and* $\delta > \delta_c$. However, in a first attempt to construct such solutions, we ignore the effect the region of pure mixing has on the flame downstream, and thus assume the constraint Eq. 51 remains satisfied, and that the extinction criteria does not need to be modified. That is, conditions *at* the flame are assumed to be unaffected by the frozen flow region; the effect of the extinguished flame base on the flow field surrounding the flame will be taken into account. In making this assumption, the parameters δ and γ, as well as the position of the flame sheet, restricted to where $\delta \geq \delta_c$, remain as given in Eqs. 45, 46, 32.

Since the solutions of the coupling functions Eqs.11-13 remain valid independent of the existence or extinction of the flame sheet, any two of the variables T, Y_F, and Y_O may be expressed as a function of the remaining one. Therefore, again it suffices to numerically solve for the temperature. The governing equation is then

$$m\frac{\partial T}{\partial x} - \frac{\partial^2 T}{\partial x^2} - \frac{\partial^2 T}{\partial y^2} = 0. \tag{52}$$

Boundary conditions at $y = 0$ and $y = L$ are

$$\frac{\partial T}{\partial y} = 0 \tag{53}$$

while at $x = 0$,

$$\text{for } 0 \leq y \leq 1, \quad mT - \frac{\partial T}{\partial x} = mT_J; \quad \text{for } 1 \leq y \leq L, \quad mT - \frac{\partial T}{\partial x} = mT_{O0}. \tag{54}$$

The condition of boundedness as $x \to \infty$ will be replaced by a condition on the truncated domain that at $x = x_{max}$,

$$\frac{\partial T}{\partial x} = 0. \tag{55}$$

Conditions at the flame front, combining Eqs. 34, 36, and 37, are finally given by

$$\text{for } \delta \geq \delta_c \text{ and } F = 0^-, \quad T = T_f - \epsilon S_F \tag{56}$$

$$\text{for } \delta \geq \delta_c \text{ and } F = 0^+, \quad T = T_f - \epsilon S_X \tag{57}$$

where $F(x, y)$, δ and γ remain as given in Eqs. 32, 45, and 46.

Solution of the Asymptotic Model

The system Eqs. 52-57 requires solution of a steady-state elliptic equation. We have solved the system by a simple five-point finite-difference scheme using Gauss-Seidel iteration. Discretization errors are thus of $\mathcal{O}(dx^2)$, where we have taken $dy = dx$. Near the flame boundary $F(x, y) = 0$, the discretization scheme has been modified to account for situations in which the flame does not exactly fall on grid points; errors near this boundary therefore may be slightly larger.

Typical solution contours are shown in Figure 7. Here $T_J = T_{O0} = 0.1$, $X_{O0} = 1.0$, $m = 9.0$, $\epsilon = 0.072$ ($\theta = 5.0$), $\Lambda = 1.0$, $L = 10.0$, and $dx = dy = 0.02$. The initial condition for the iteration was taken from the Burke-Schumann solution for $x > x_c$ and the initial ($x = 0$) condition for $x < x_c$. Profiles show a liftoff height of between one and two jet diameters, and are in fairly good qualitative agreement with previous experimental and numerical studies [7]. Figure 7 is qualitatively similar to Figure 2 obtained from the numerical solution. In the fully numerical solution, however, the flame width, particularly at the base, appears broader than in Figure 7, in which the flame is assumed to be confined to a surface. However, this broader flame width is consistent with a smaller effective Damköhler number at the flame base. Note also that while liftoff heights are comparable in the two figures, they are obtained for largely disparate values of Λ (or D.)

Figure 8 shows the effect of the mass flow rate on the flame shape. Here solutions of $F(x, y) = 0$, $\delta \geq \delta_c$ are shown for several values of m, with $T_J = T_{O0} = 0.1$, $X_{O0} = 2.0$ $L = 10.0$, $\Lambda = 2.0$, $N = 200$. As m is increased, the liftoff height of the flame and the overall flame height increase. The length of the flame (the distance from the lifted base to the flame tip) increases as well. In Figure 9, flame shapes for the same parameters, but a smaller value of the ambient oxidant concentration $X_{O0} = 0.5$, are shown. The liftoff and flame heights exhibit the same general trends as in Figure 8. However, for the smaller values of X_{O0}, liftoff heights are shorter, flame lengths are longer, and flame shapes are wider and more rounded.

In Figure 10, liftoff heights are shown versus m for several values of the parameter Λ. Here $X_{O0} = 1.0$, with $T_J = T_{O0} = 0.1$, $L = 10.0$, and $N = 200$. As expected, liftoff heights decrease as Λ increases, consistent with the Burke-Schumann limit $\Lambda \to \infty$ in which flames are attached for all values of m. In Figure 10 the flame height, which does not vary with Λ in the current approximation, is also shown, and increases linearly with m. Flame height predictions from the asymptotic model are compared with predictions from the numerical model in Figures 3 and 4.

The results from the asymptotic model show some qualitative agreement with the numerical formulation results. Liftoff heights predicted using the asymptotically-derived extinction criteria increase with jet exit velocity and decrease as the Damköhler number is increased. However, we see a linear, rather than faster-than-linear, increase in liftoff height with flow rate m. Also, for a given value of Λ, liftoff height predictions from the numerical formulation are much higher than those from the asymptotic model. This suggests that for a lifted flame, coupling between the frozen flow region adjacent to the jet exit and the lifted flame base is significant. This is reasonable since heat loss at the flame edge due to the adjacent cold region would reduce the effective Damköhler number there, thus resulting in an underprediction of lift-off height. It is reasonable to think that if coupling were included in the asymptotic model, the cold flow region near the jet would tend to expedite extinction of the adjacent flame base, and thus a faster-than-linear dependence of liftoff

height on flow rate would result, along with better quantitative agreement. However, that the asymptotic model cannot account for partial premixing effects also might be contributing to the discrepancy. A modification of the analysis to account for some degree of premixing would likely modify the extinction criteria Eq. 48 and also might lead to better agreement between the two models. While lift-off height predictions of the two models are different, we note that the *flame* heights predicted by both models show excellent agreement.

Because the flame heights predicted by the two models agree, and the general liftoff trend of increasing height with increasing flow rate and decreasing Damköhler number exists in both models, we investigate further whether an extinction mechanism plays a role in laminar diffusion flame lift and stabilization. In the asymptotic model, we obtain an extinction criterion that says a flame may exist only for

$$\Lambda \geq \delta_c (1 + X_{O0})^2 \left(\left(\frac{\partial S}{\partial x} \right)^2 + \left(\frac{\partial S}{\partial y} \right)^2 \right) \Bigg|_{F=0} . \tag{58}$$

Now the extinction parameter Λ involves primarily the Damköhler number D and the activation energy θ (recall $\Lambda = 4T_f^4 De^{-\theta/T_f}/\theta^3$.) We therefore investigate whether results from the numerical formulation correlate with this asymptotically-derived extinction parameter. In Figure 11, Eqs. 14-17 were solved to obtain curves of liftoff heights versus m for identical values of Λ. Here the values of D and θ vary greatly between curves, but have been chosen such that in all curves they combine so that Λ is fixed at the value $\Lambda = 40.0$. The results show that as the scaled activation energy θ is increased, the curves coalesce. Since the asymptotic model was derived in the limit of large activation energy, one expects that as this parameter is increased, solutions should begin to converge to a single solution. In the present results, this means that if results correlate with respect to the parameter Λ, as it is held fixed and θ is increased, the curves of lift-off height versus m should begin to coalesce. Since Figure 11 shows that this coalescing appears to take place, our results suggest that the parameter Λ derived from the asymptotic analysis is indeed a parameter which characterizes flame lift.

DISCUSSION

Experiments indicate that for low jet velocities, diffusion flames are attached to the jet nozzle. As the flow velocity is increased, such flames may lift off of the nozzle, so that the flame base is located several jet diameters downstream. As the flow velocity is increased further, blow out occurs and the flame is extinguished. Lee et al. [9] suggest that, depending on the fuel type, degree of dilution, and the nozzle diameter, liftoff and blowout may both occur in the laminar regime, or liftoff may occur in the laminar regime with blowout occurring after the transition to turbulence, or liftoff and blowout may both occur only after a transition to turbulence. While there have been many experimental and numerical studies of diffusion flame liftoff and blowout in turbulent regimes, fewer studies exist which investigate laminar flame lift.

Experiments involving laminar propane jet diffusion flames by Lee et al. [9] suggest that liftoff heights increase as the jet exit velocity of the propane is increased, at a faster-than-linear rate. Flame heights increase linearly with an increase in the nozzle exit velocity, with the flame length (distance from the lifted base to flame tip) approaching zero at blowout. When the fuel jet was diluted, the liftoff height increased for a fixed value of the jet velocity. Lee and Chung [6] have also investigated the effect of a low velocity oxidant coflow on a propane jet diffusion flame. Such a coflow has a minimal effect on attached flame length, but results in a larger liftoff height. Liftoff and blowout of the jet flame occur at lower fuel jet velocities when there is a coflow. Chung and Lee [20], [6], in a cold jet analysis similar to that of Savas and Gollahalli [8], also have derived

analytical expressions for liftoff heights, based on the assumption that a lifted flame at its base is fully premixed. They postulate that a lifted flame is stabilized along the stoichiometric contour where the (cold) flow velocity equals the appropriate burning velocity of the premixture. Lifted laminar diffusion flames were also observed in experiments and numerical simulations by Xu et al. [7]. They considered a circular jet geometry with an equal velocity oxidant coflow, using detailed chemistry and complex transport models in their numerical simulation. Their results show a lifted flame in which profiles of the temperature, fuel, and oxidant are qualitatively similar to the profiles shown in Figures 2 and 6; liftoff height trends with respect to system parameters were not discussed.

The results from the numerical model show good qualitative agreement with such experimental results. Liftoff height trends shown in Figure 3 are qualitatively the same as those described by Lee et al. [9]. Profiles of temperature and fuel and oxidant mass fraction from the numerical model are very comparable to those obtained by Xu et al. [7], and profiles from the asymptotic model are comparable to such results as well. Both the current calculations and the calculations of Xu et al. show the existence of "wings" of fuel outside of the core of the fuel jet at the flame base, for example. In the current work these wings are more pronounced than in [7]; however, this is likely attributable to the use of a planar jet as compared to the circular jet of Xu et al., and to the exclusion of a radial velocity component. Flame heights predicted by the numerical and asymptotic models show excellent agreement. That the numerical results appear to correlate with the extinction parameter Λ from the asymptotic analysis suggests that diffusion flame extinction plays a role in lifted flame stabilization.

It is useful to again analyze the results in light of the flame stabilization theory proposed by Chung and Lee [6]. They hypothesize that flame stabilization occurs along the stoichiometric contour where a cold flow velocity balances the stoichiometric burning velocity. In the present model, we consider only a one-dimensional, axial flow velocity. As a result, the velocity of a cold flow is constant everywhere in the flow field. A premixed flame base theory then suggests that the model should result in a stabilized lifted flame only if the fuel and oxidant source velocities are equal to an appropriate premixed burning velocity; in this case, the flame stabilization point would be indeterminate, since at every point along the stoichiometric contour the velocity is the same. However, in the calculations we obtain unique, stabilized lifted flames for multiple flow inlet velocities. This suggests that a propagating, fully premixed flame base theory cannot fully explain flame stabilization.

Our results also should be discussed with respect to partial premixing analyses, [16], [17], [18], such as those of edge-flames and triple flames. In many analyses of this type of phenomena, the domain is considered to be unbounded and an infinite region of partial premixing exists. In such scenarios it seems reasonable to equate a flame stabilization point with the location at which a flow velocity equals an appropriately calculated edge-flame, or partially premixed flame, propagation velocity. In the work of Buckmaster [16] and in that of Müller et al. [17], for example, expressions for such partially premixed flame velocities are described in which the propagation velocity is dependent on the scalar dissipation rate (which is inversely proportional to our effective Damköhler number δ.) While our results affirm the importance of this parameter, they cannot be fully explained by such a stabilization theory even when dependence of the flame speed on scalar dissipation is taken into account. This is in part because, as the scalar dissipation rate decreases and the effective Damköhler number increases towards infinity, such analyses reduce to a fully premixed flame edge description. While such a result may be reasonable and appropriate in the respective models considered, clearly in the jet flame model of the present work, the infinite Damköhler limit corresponds to a non-propagating, attached Burke-Schumann flame. Thus while we cannot rule out the possibility of partially premixed flame propagation contributing to lifted flame stabilization,

such theories currently cannot provide a full description of the phenomena.

CONCLUSIONS

A numerical solution of a planar jet flame and a flame sheet model, in the limit of large activation energy and large Damköhler number, were used to investigate liftoff of laminar diffusion flames. The numerical results are qualitatively consistent with experiments [9] and more complex numerical simulations [7]. Some agreement also exists between experiments and the asymptotic formulation results; inclusion of coupling and heat loss effects between the frozen region below the flame base and the flame itself in this model should produce improved agreement. Discrepancies between the two models may be attributable to the need to modify the extinction condition to account for flame edge effects. That the numerical model investigated here is very simple and yet still shows good qualitative agreement with experiments suggests that at least some of the physical processes responsible for flame lift are correctly accounted for in the model. In particular, we note that while it is true that "real" jet flames have two (or three) dimensional velocity fields, it is interesting that in our numerical work we are able to obtain lifted flames and triple flame structures with only a one-dimensional velocity field. Thus while the inclusion of multidimensional effects would modify our liftoff results, it is more significant that our work clearly shows that flow redirection at the flame base is not necessary to obtain triple flame structures or flame stabilization: The simplicity of our numerical model in this context produces insight which a more complicated numerical scheme might be incapable of providing.

Local diffusion flame extinction is shown to be a plausible contributing mechanism of flame lift. A simple description of flame stabilization occurring where the flow velocity balances a premixed burning velocity is found to be inadequate. However, the possibility of some degree of premixed burning affecting the flame structure and stabilization is not excluded; rather, it is shown that such burning does not appear to be the sole controlling mechanism of flame lift.

In turbulent flames, Kaplan et al. [19] have used detailed numerical simulations of the full Navier-Stokes equations to investigate flame lift. Their results corroborate parts of both the flame extinction and premixedness theories, in a turbulent flame context. While a turbulent flow field may significantly alter the dynamics of flame stabilization, a full solution of the Navier-Stokes equations in a laminar regime in which buoyancy and a multidimensional velocity field are accounted for also could somewhat modify the flame liftoff results obtained here.

ACKNOWLEDGEMENTS

This work was performed while S. Cheatham held a National Research Council - Naval Research Laboratory Research Associateship.

References

[1] Vanquickenborne, L. and van Tiggelen, A., *Combustion and Flame* 10:59-69 (1966).

[2] Kalghatgi, G.T., *Combustion Science and Technology* 41:17-29 (1984).

[3] Peters, N., *Progress in Energy and Combustion Sciences* 10:319-339 (1984).

[4] Peters, N. and Williams, F.A., *AIAA* 21, No. 3, 423-429, (1983).

[5] Pitts, W.P., *Twenty-Second Symposium (International) on Combustion*, The Combustion Institute, 809-816, (1988).

[6] Lee, B.J. and Chung, S.H., *Combustion and Flame* 109:163-172 (1997).

[7] Xu, Yuenong, Smooke, M.D., Lin, P., and Long, M.B., *Combustion Science and Technology* 90:289-313 (1993).

[8] Savas, O. and Gollahalli, S.R., *Journal of Fluid Mechanics* 165:297-318 (1986).

[9] Lee, B.J., Kim, J.S. and Chung, S.H., *Twenty-Fifth Symposium (International) on Combustion*, The Combustion Institute, 1175-1181 (1994).

[10] Wichman, I.S. and Ramadan, B., *Physics of Fluids* 10 No. 12, 3145-3154 (1998).

[11] Buckmaster, J. and Matalon, M., *Twenty-Second Symposium (International) on Combustion*, The Combustion Institute, 1527-1535 (1988).

[12] Liñán, A. and Crespo, A., *Combustion Science and Technology* 14:95-117 (1976).

[13] Buckmaster, J. and Weber, R., *Twenty-Sixth Symposium (International) on Combustion*, The Combustion Institute, 1143-1149 (1996).

[14] Chung S.H. and Law C.K., *Combustion Science and Technology* 37:21-46 (1984).

[15] Liñán, A., *Acta Astronautica* 1:1007-1039 (1974).

[16] Buckmaster, J. *Journal of Engineering Mathematics*, 31:269-284 (1997).

[17] Müller, C.M., Breitbach, H. and Peters, N., *Twenty-Fifth Symposium (International) on Combustion*, The Combustion Institute, 1099-1106 (1994).

[18] Daou, J. and Liñán, A., *Combustion Theory and Modelling*, 2:449-477 (1998).

[19] Kaplan, C.R., Oran, E.S. and Baek, S.W., *Twenty-Fifth Symposium (International) on Combustion*, The Combustion Institute, 1183-1189 (1994).

[20] Chung, S. H. and Lee, B.J., *Combustion and Flame*, 86:62-72 (1991).

[21] Higuera, F.J. and Liñán, A., *Journal of Fluid Mechanics* 329:389-411 (1996).

[22] Gerald, C.F. and Wheatley, P.O., *Applied Numerical Analysis*, 4th Ed., Addison-Wesley Publishing Company, Inc. (1989).

[23] Jia, X. and Bilger, R.W., *Combustion Science and Technology* 99:371-376 (1994).

[24] Cheatham, S. and Matalon, M., *Journal of Fluid Mechanics* 414:105-144 (2000).

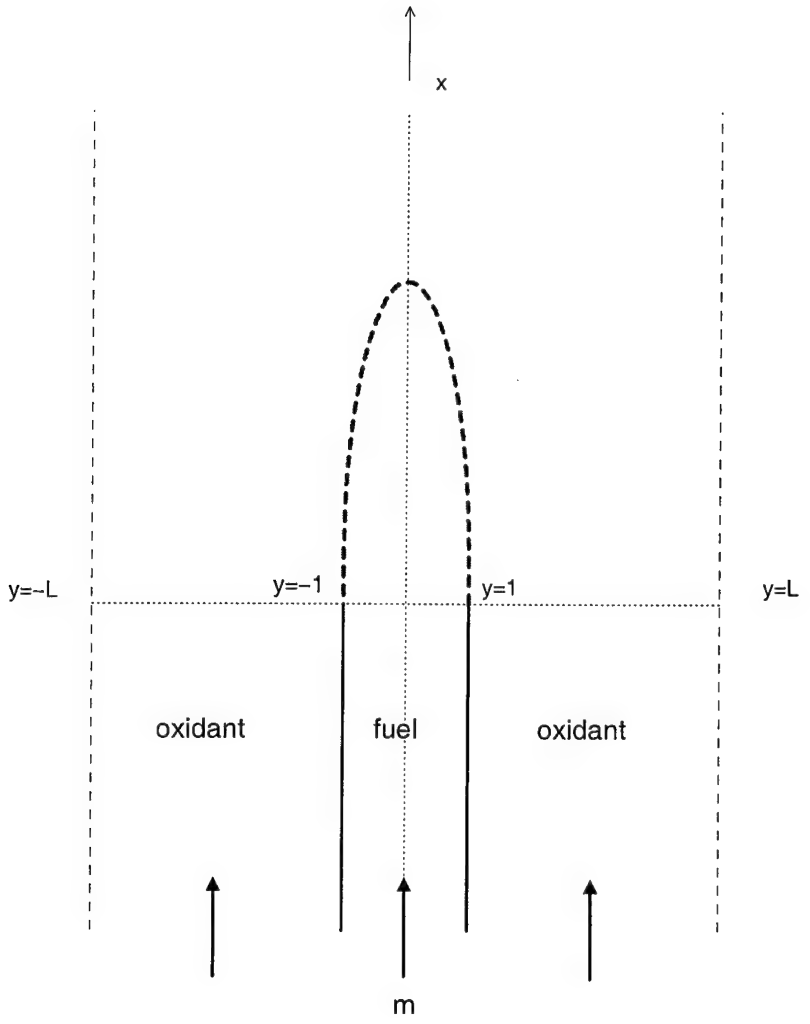

Figure 1: Geometry of the flow field.

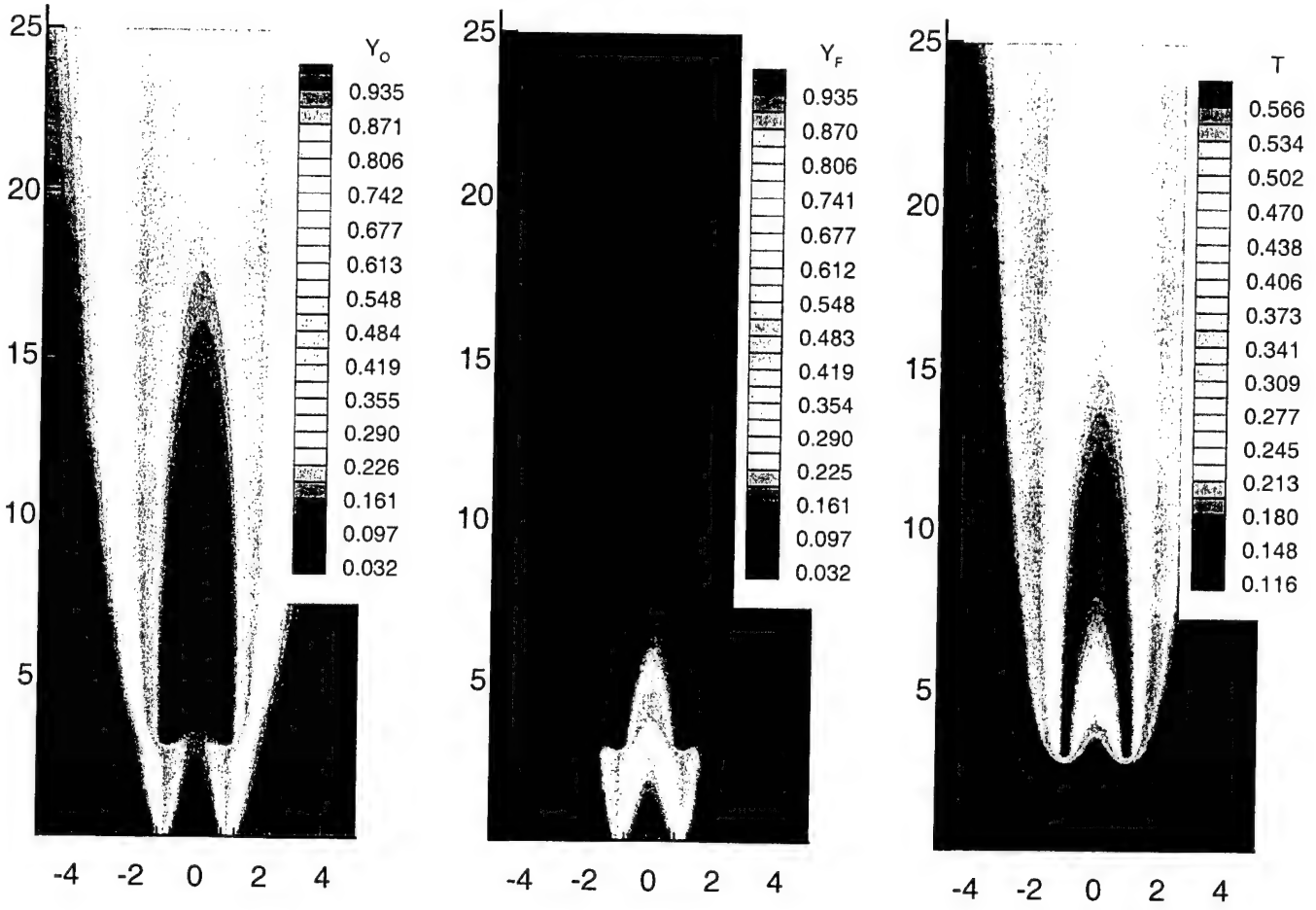

Figure 2: Solution contours of the oxidant and fuel mass fractions and the temperature from the numerical model; $m = 9.0$, $T_J = T_{O0} = 0.1$, $X_{O0} = 1.0$, $L = 10$, $dx = dy = 0.02$, $N = 200$, $D = 4 \times 10^7$, and $\theta = 5.0$ ($\Lambda = 40$).

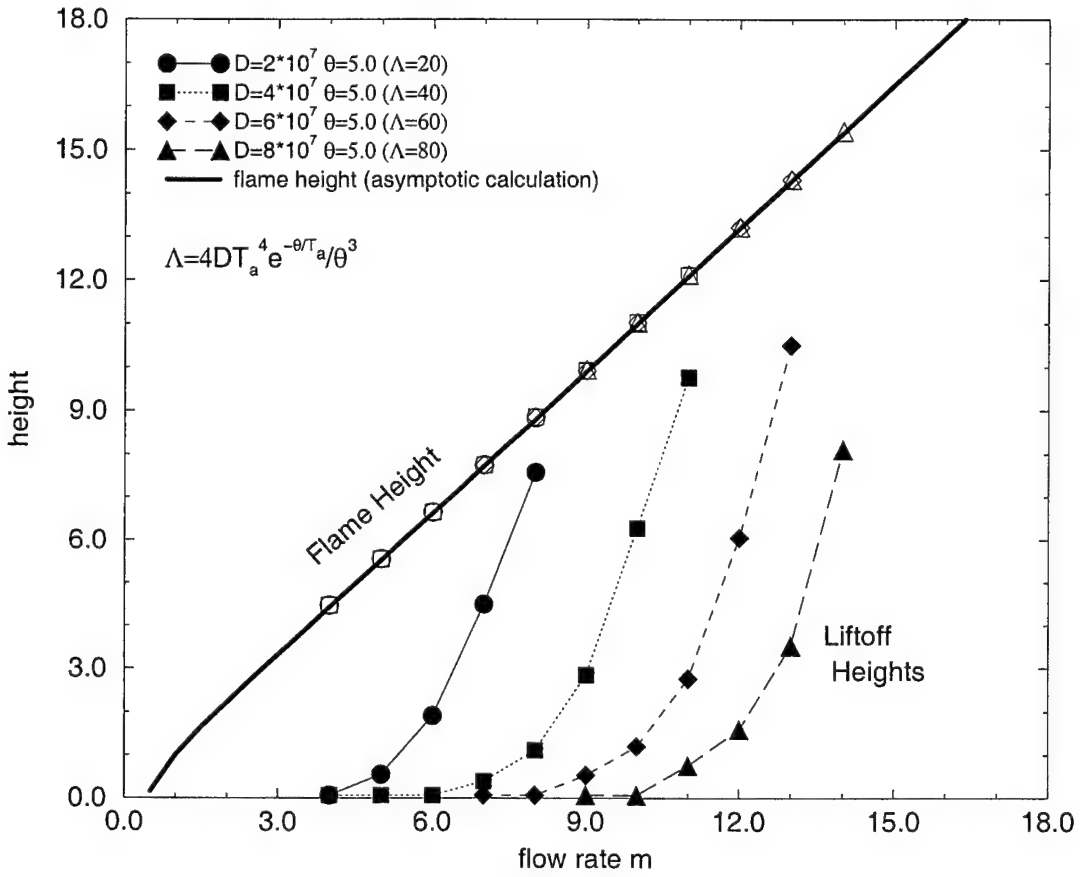

Figure 3: Liftoff and flame heights versus the flow rate m for several values of D. Predictions are from the numerical model, with $T_J = T_{O0} = 0.1$, $X_{O0} = 1.0$, $L = 10.0$, $\theta = 5.0$, and $N = 200$.

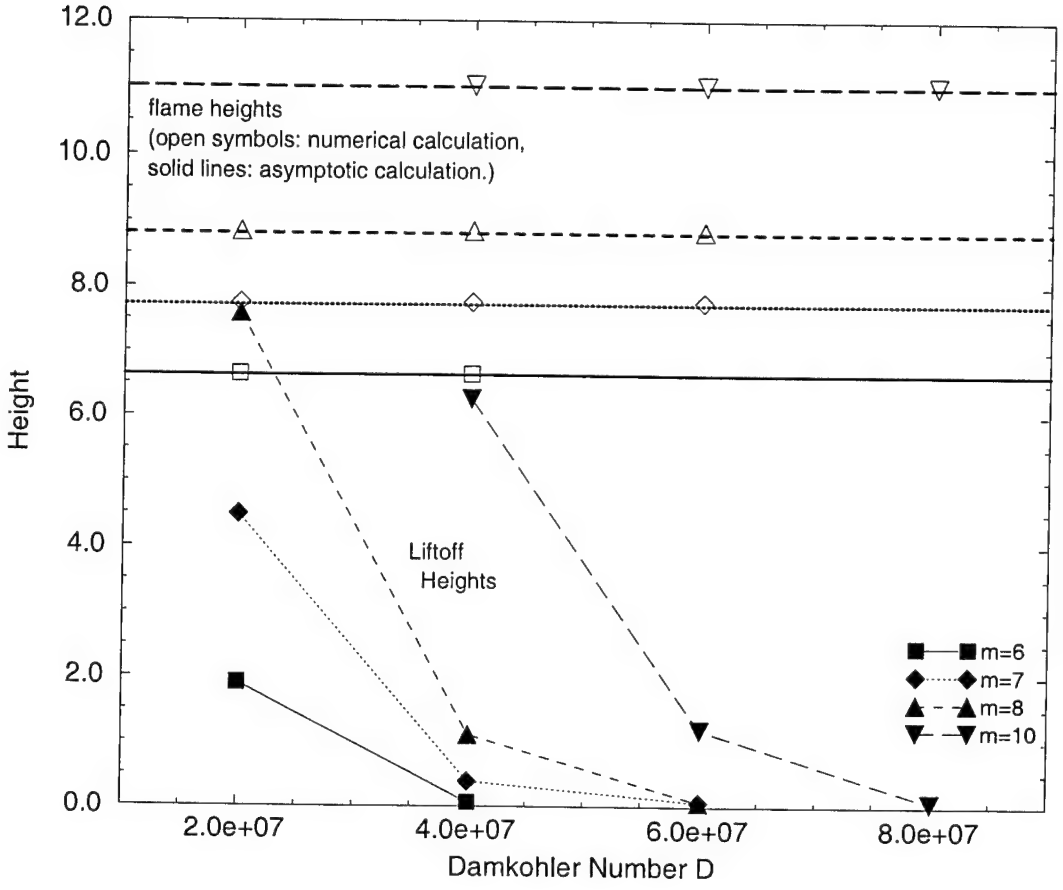

Figure 4: Liftoff and flame heights versus D for several values of the flow rate m. Predictions are from the numerical model, with $T_J = T_{O0} = 0.1$, $X_{O0} = 1.0$, $L = 10.0$, $\theta = 5.0$, and $N = 200$.

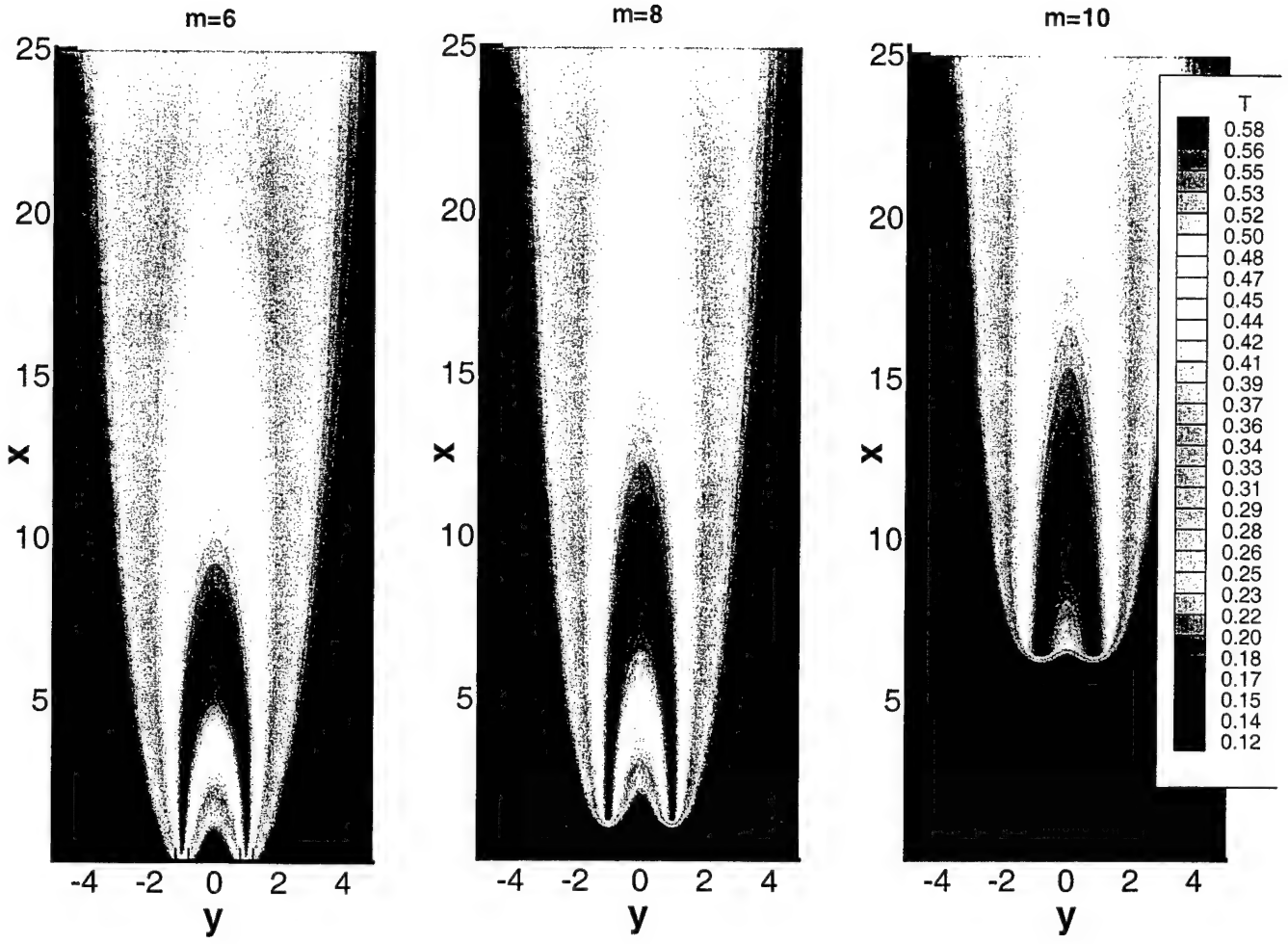

Figure 5: Temperature contours from the numerical model for $m = 6, 8$, and 10, with $T_J = T_{O0} = 0.1$, $X_{O0} = 1.0$, $L = 10.0$, $D = 4 \times 10^7$ and $\theta = 5.0$ ($\Lambda = 40$), and $N = 200$.

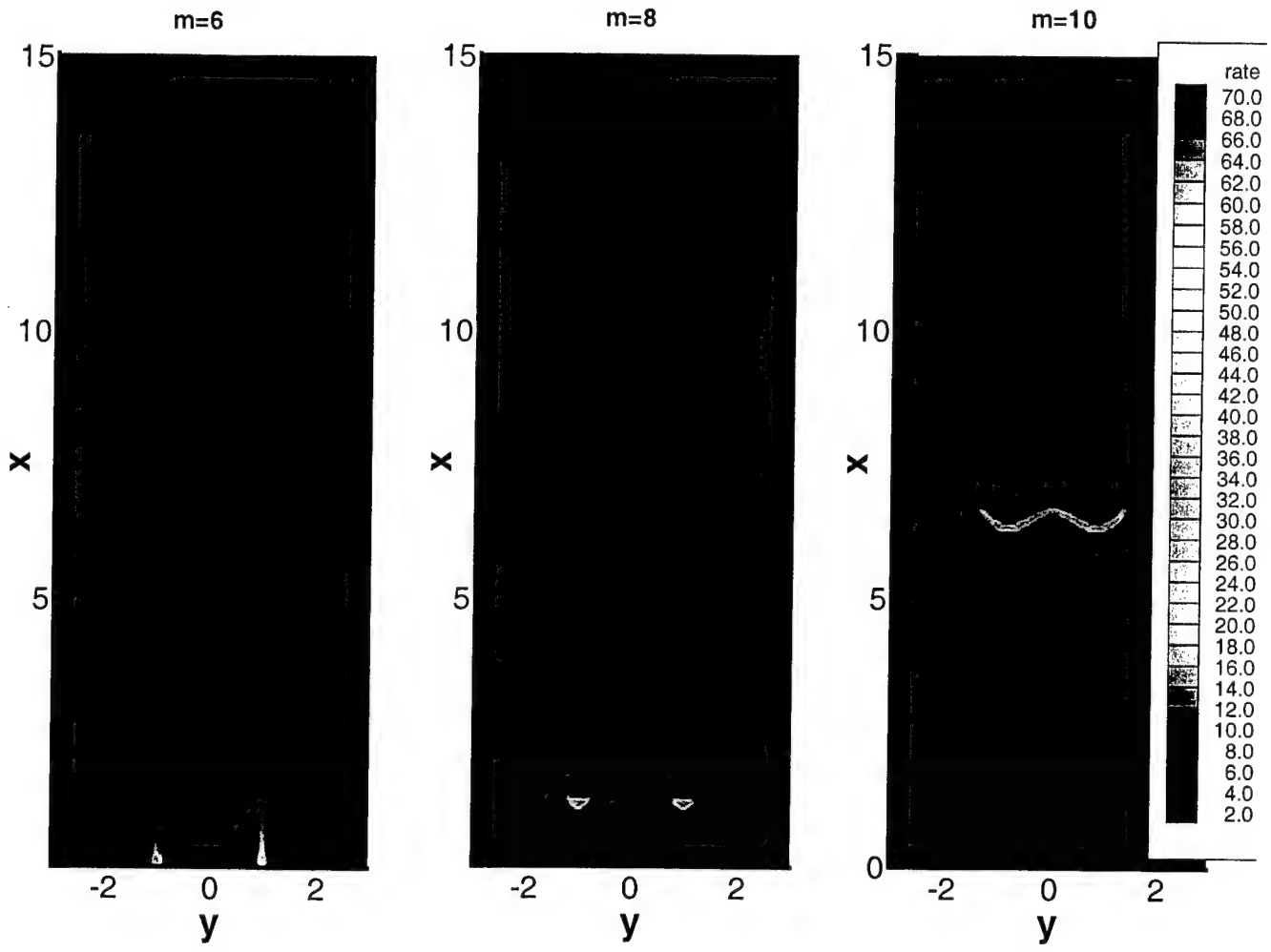

Figure 6: Contours of the reaction rate, for $m = 6$, 8, and 10, with $T_J = T_{O0} = 0.1$, $X_{O0} = 1.0$, $L = 10.0$, $D = 4 \times 10^7$ and $\theta = 5.0$ ($\Lambda = 40$), and $N = 200$.

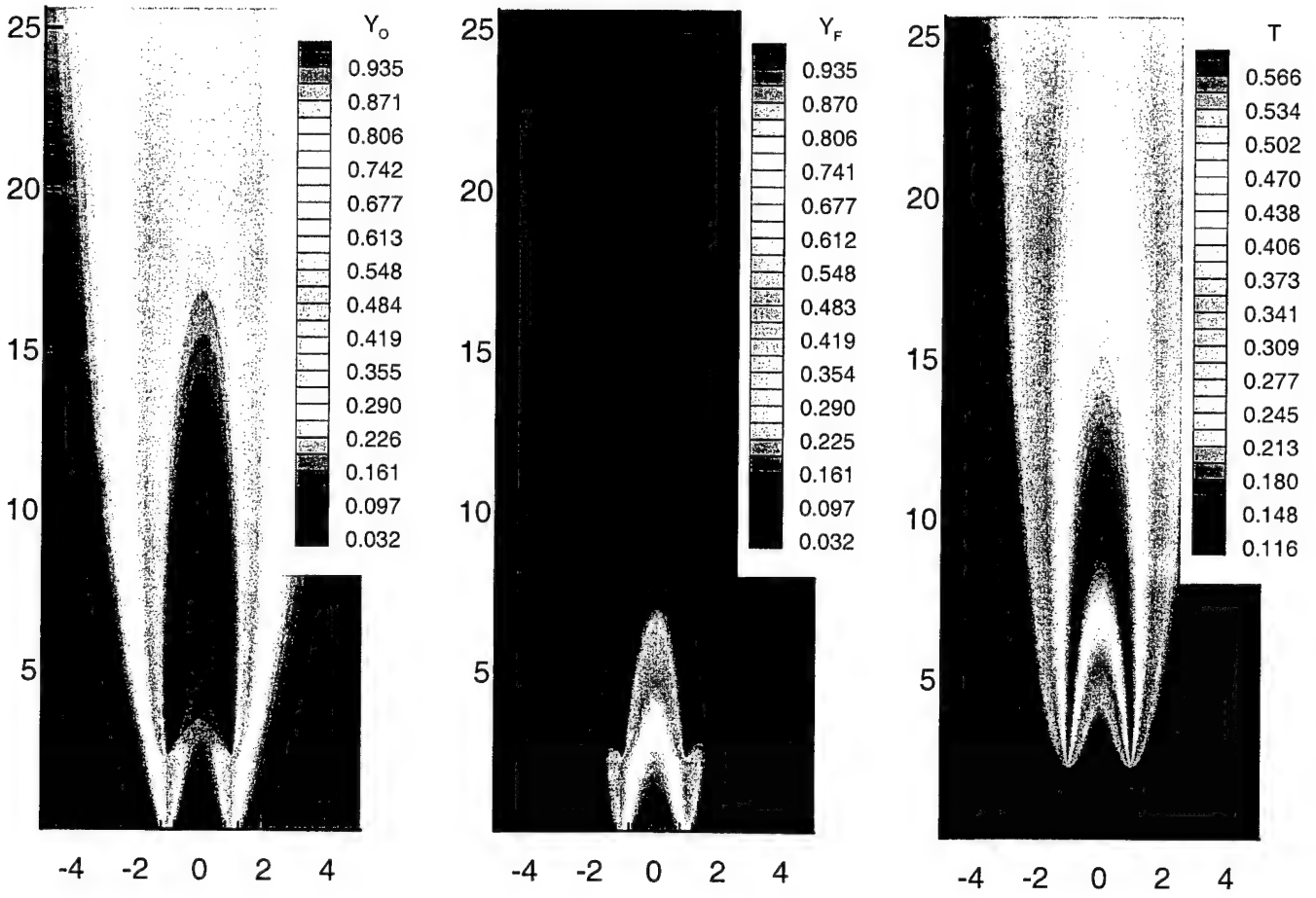

Figure 7: Solution contours of the oxidant and fuel mass fractions and the temperature; $m = 9.0$, $T_J = T_{O0} = 0.1$, $X_{O0} = 1.0$, $\epsilon = 0.072$ $(\theta = 5)$, $\Lambda = 1.0$, $L = 10$, $dx = dy = 0.02$, and $N = 200$.

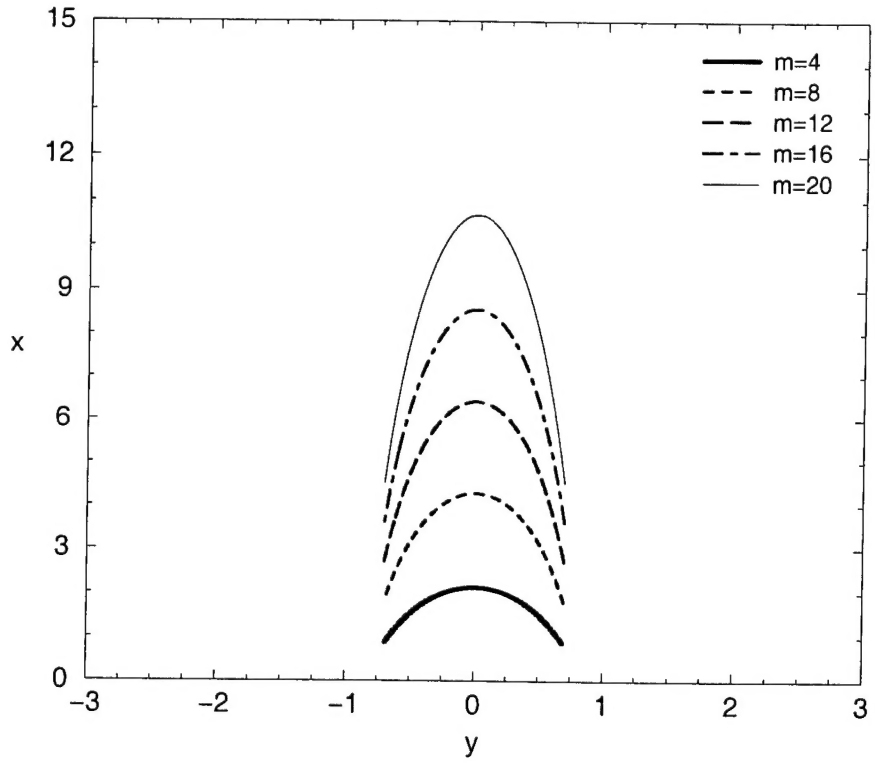

Figure 8: Flame shapes for several values of m, with $T_J = T_{O0} = 0.1$, $X_{O0} = 2.0$, $L = 10.0$, $\Lambda = 2.0$, $N = 200$.

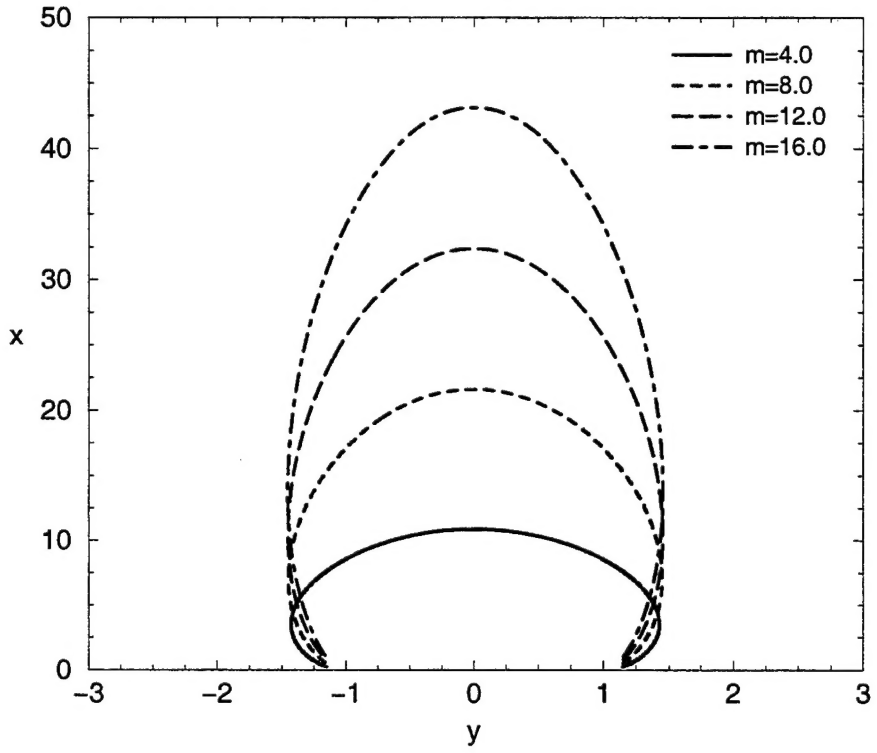

Figure 9: Flame shapes for several values of m, with $T_J = T_{O0} = 0.1$, $X_{O0} = 0.5$, $L = 10.0$, $\Lambda = 2.0$, $N = 200$.

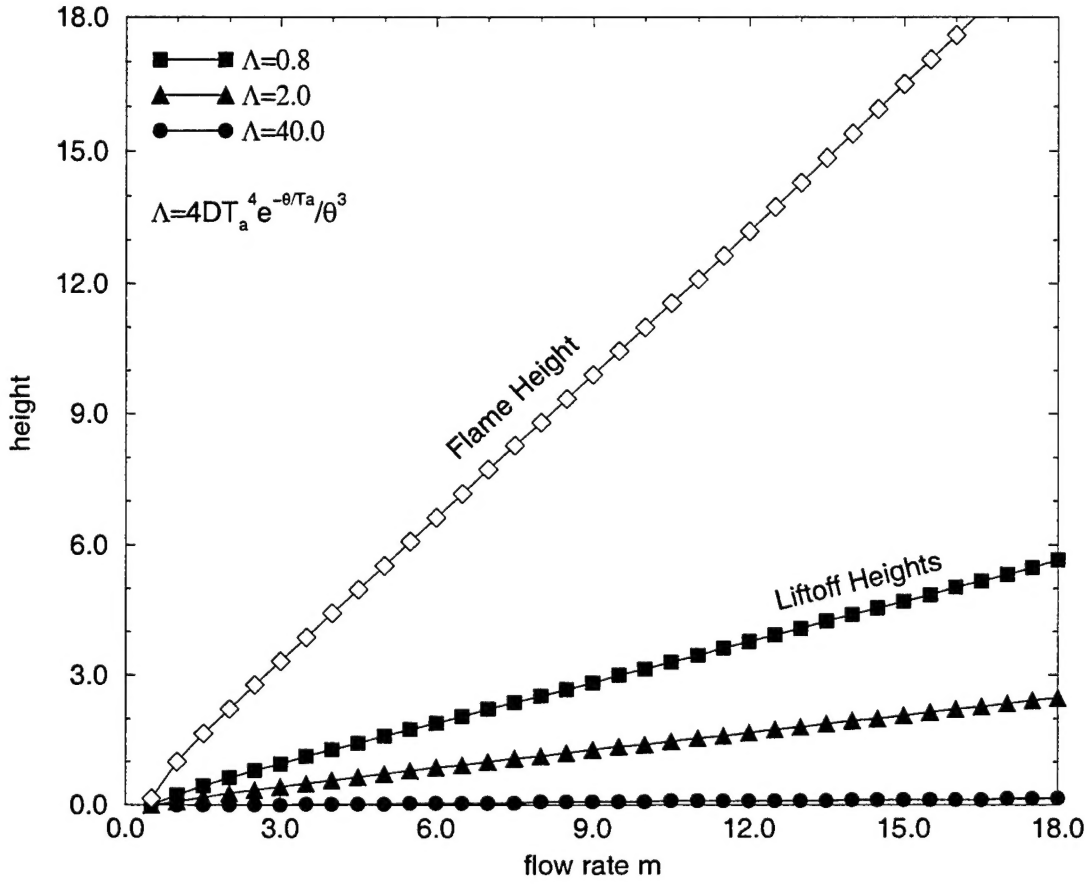

Figure 10: Predictions of liftoff and flame heights from the asymptotic theory, with $T_J = T_{O0} = 0.1$, $X_{O0} = 1.0$, $L = 10.0$, and $N = 200$.

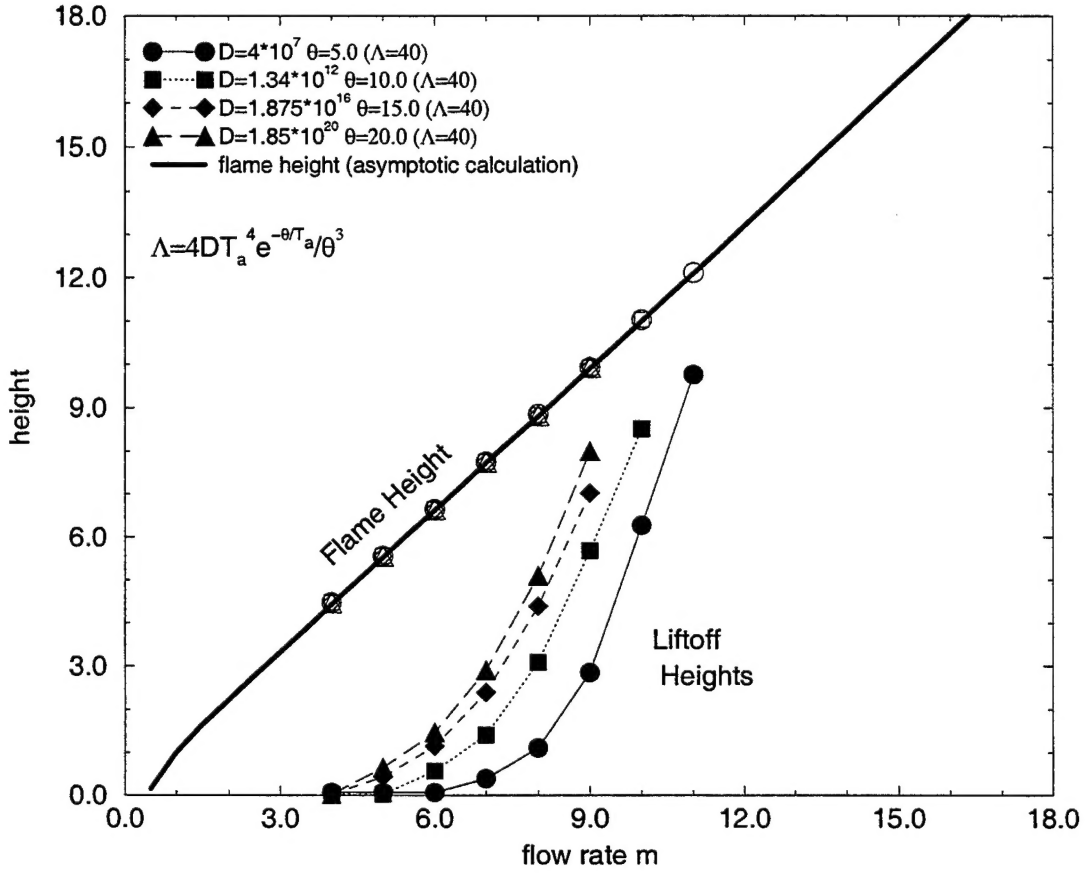

Figure 11: Liftoff and flame heights versus m with $\Lambda = 40.0$, for $T_J = T_{O0} = 0.1$, $X_{O0} = 1.0$, $L = 10.0$, $N = 200$, and several values of D, θ.